Journal of Hydrology: Regional Studies 47 (2023) 101382

Contents lists available at ScienceDirect

Journal of Hydrology: Regional Studies

journal homepage: www.elsevier.com/locate/ejrh

The role of physical geography on Puerto Rico's water budget

Flávia D.S. Moraes [a,*,1], Thomas L. Mote [a], Todd C. Rasmussen [b]

[a] Department of Geography, University of Georgia, Athens, GA 30602–5026, USA
[b] Warnell School of Forestry and Natural Resources, University of Georgia, Athens, GA 30602–2152, USA

ARTICLE INFO

Keywords:
Drought
Water stress
Tropical climate
Puerto rico
Caribbean islands

ABSTRACT

Study region: Puerto Rico, a tropical island in the Caribbean Sea.
Study focus: This study examines how water stress in Puerto Rico is influenced by its physical geography using a new USGS Soil-Water-Balance Model (Version 2.0) applied to three periods: a baseline climatology (1981–2010), a recent decade (2010–2019), and multiple drought years (1991, 1994, 1997, 2015).
New hydrological insights for the region: Oceanic islands often experience chronic water stress due to their size, population, land use, and geomorphology. Yet more severe, acute stress arises due to atmospheric forcing droughts, in which decreased precipitation is accompanied by increased temperatures, evapotranspiration, and water withdrawals. Based on our analysis of the physical geography of Puerto Rico, we find that water stress is more likely in southern Puerto Rico during both baseline and recent decade conditions due to reduced net infiltration within the rain shadow of the Cordillera Central. On the contrary, chronic stress is lower in mountainous and vegetated areas on the remainder of the island, as well as where coastal aquifers are available for augmenting surface water. During drought events, water stress is more common in central and eastern Puerto Rico mainly due to reductions in precipitation and net infiltration, increased evapotranspiration, and limited groundwater availability. Drought imposes additional chronic stresses by reducing recharge to coastal aquifers. These coastal aquifers are recharged by direct rainfall and streamflow from central Puerto Rico; the decreased precipitation and net infiltration in those areas constrain water availability during drought.

1. Introduction

The insular Caribbean has great cultural diversity among the islands, but the region shares similarities regarding its rich biodiversity, including but not limited to tropical rain forests, endemic species, and coral reefs (Geoghegan and Renard, 2002). However, this rich environment has limited water resources due to the islands' small sizes, geomorphic characteristics, and prevailing climate.

Geological composition affects water availability because topography and geology play critical roles in the physiographic control of rainfall patterns and the availability of surface and subsurface water (Hendry, 1996). In the Caribbean carbonate islands, most of the water resources are located within the subsurface, while the limited amount of surface water is frequently hypersaline because of high evaporative demand. Therefore, these islands are particularly vulnerable to drought as rainwater catchments and groundwater freshwater lenses are the main water-supply options, and both rely on rainfall-driven recharge (Cant, 1996; Falkland, 1999). Water

* Corresponding author.
E-mail address: fmoraes@gsu.edu (F.D.S. Moraes).
[1] Present address: Department of Geosciences, Georgia State University, 38 Peachtree Center Ave SE 7th Floor, Suite 733, Atlanta, GA 30303, USA

https://doi.org/10.1016/j.ejrh.2023.101382
Received 10 March 2022; Received in revised form 20 January 2023; Accepted 6 April 2023
Available online 18 April 2023

supplies on volcanic islands, on the other hand, are usually obtained from surface sources due to limited percolation, steep terrain, and high runoff (Hendry, 1996). Additionally, the topography of the islands can also affect the magnitude and the location of rainfall, with orographic uplift from the mountains resulting in more rainfall occurring on the windward side of Caribbean islands (Jury, 2020; Martinez et al., 2019; Sobel et al., 2011).

The geology, topography, climate, and lack of economic diversity in the insular Caribbean make drought one of the most frequent climate hazards, resulting in economic losses and water shortages (Farrell et al., 2010). The seasonal rainfall variability and the physical geography of the Caribbean limit the ability to capture water during rainy seasons and retain it during dry seasons and multi-year drought events. Consequently, many islands experience problems in meeting water demand during drier periods of the year (Ault, 2016; Cashman et al., 2010; Holding et al., 2016).

A significant drying trend has occurred in the Caribbean since 1950, and drought is expected to be more frequent and severe in the Caribbean (Cashman et al., 2010; Herrera et al., 2018; Karnauskas et al., 2018; Moraes et al., 2022). Predictions based on projected changes in climate also indicate that freshwater stress will be one of the main environmental concerns for small island states until the end of the century (Karnauskas et al., 2018). Understanding the water balance is important for predicting the effects of long-term climate change on oceanic islands in tropical climates. This knowledge is vital for preparing local governments as water stress increases over time.

Therefore, this work focused on the main island of Puerto Rico as a case study in the insular Caribbean. The island is used to examine the role of physical geography on water-budget components, including potential groundwater recharge, comparing a baseline period and multiple-drought years. Puerto Rico is part of the Greater Antilles in the Caribbean Sea, rising from sea level to 1075 m high at the top of the Luquillo Mountains over a distance of only 10–20 km along its east coast (Garcia-Martino et al., 1996). Together with the extreme climatic events that affect the island, the mountainous landscape introduces complexities related to variations in soils, vegetation, and rainfall.

Past studies analyzing the hydroclimatic characteristics of Puerto Rico have focused on understanding the hydrological consequences of major hurricanes (Miller et al., 2019), the precipitation variability (Keellings and Hernández Ayala, 2019; Ramseyer and Mote, 2018), the historical and projected climate change (Jury, 2022), as well as the spatial-temporal variability of meteorological drought events on the island (Sorí et al., 2021) and the connection between drought and the Saharan air layer (Miller et al., 2021; Mote et al., 2017). Recent studies have used water-budget models to predict local hydrology within the rainforest area of the Luquillo Mountains (Zhang et al., 2018), understand the role of vegetation on streamflow (Hall et al., 2022), and characterize island-wide hydrology (Harmsen et al., 2021).

However, there is a gap in the literature regarding the use of high-resolution model to understand how the island's physical

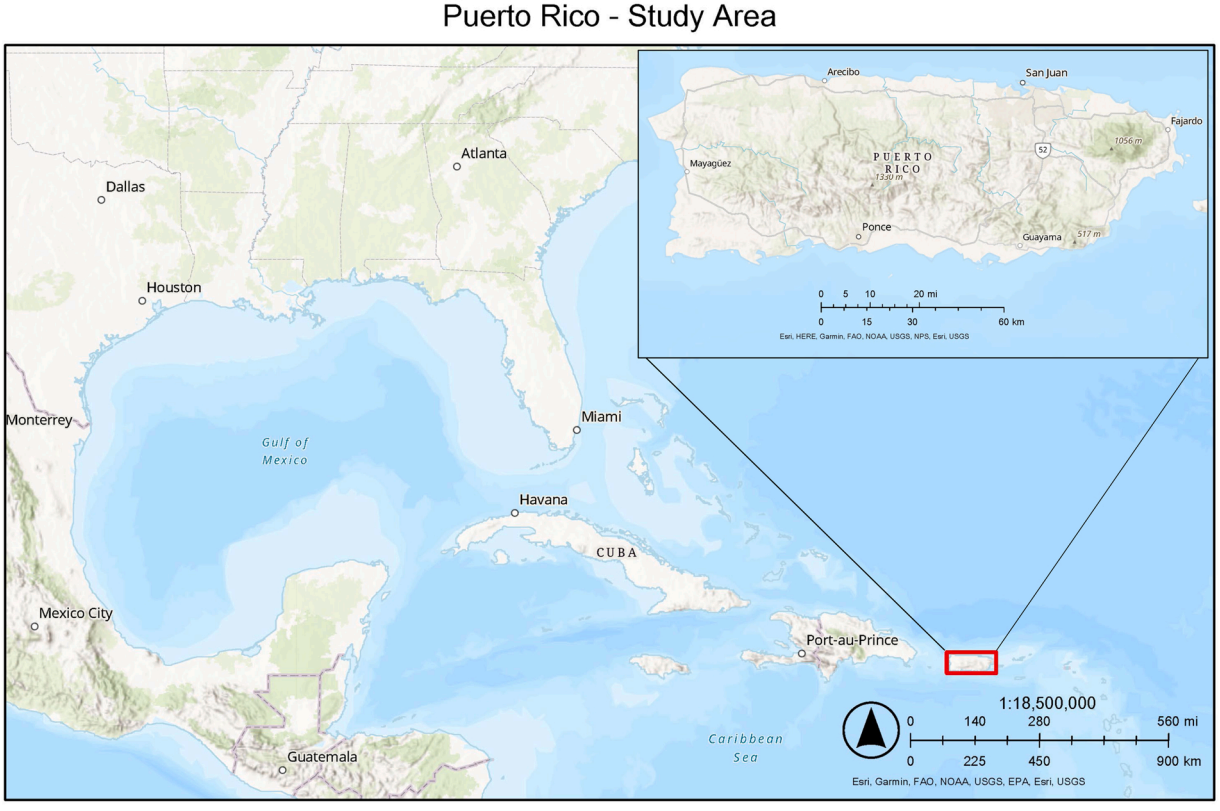

Fig. 1. Puerto Rico study area map and location.

geography (e.g., topography, soils, climate) affects its water balance island-wise, especially during periods drought. Therefore, this work reduces that gap by applying the newly released, open-access, Soil-Water-Balance model (SWB2, Version 2.0) developed by the U.S. Geological Survey (Westenbroek et al., 2018), to analyze the temporal and spatial variability in Puerto Rico's water balance and potential groundwater recharge. The model provided a high-resolution (300-m) platform to investigate how Puerto Rico's physical geography influences its water budget during a baseline period (1981–2010), a recent decade (2010–2019), and multiple drought years (1991, 1994, 1997, 2015). Additionally, this work provided an opportunity to evaluate model performance without first calibrating to field observations, considering many oceanic islands in tropical climates lack such information, and an opportunity to compare the results with another recently released regional model, GOES_PRWEB (Harmsen et al., 2021). By demonstrating the utility of the SWB2 model in Puerto Rico, we seek to enhance the capability of other water-stressed oceanic islands in tropical settings to assess, plan and manage their water resources.

2. Data and methods

2.1. Study area

Puerto Rico's main island is located in the western Tropical Atlantic, extends approximately 180 km from west to east and 65 km from north to south, and has a quasi-rectangular shape with an area of approximately 11,700 km^2 (Fig. 1). The main island is predominantly mountainous (53% of the area), with a maximum altitude of 1340 m above sea level. While most of the northwest coast is karstic (underlain by carbonates), the southern coast is predominantly discontinuous coastal sedimentary plains. These regions are divided by a central mountain range extending from east to west called the Cordillera Central (Mendez-Tejeda et al., 2016; Miller et al., 1997; Torres-Valcárcel et al., 2014).

Topographically driven drainage is predominantly radial from the central highlands to the sea and "consists of short, deeply incised streams that have steep gradients in the upper reaches" (Miller et al., 1997). Puerto Rico has few perennial streams (along the southern coast), and those rivers' flow requires precipitation and sustained wet periods.

Annual precipitation is also topographically driven, with orographic uplift causing rainfall variation based on elevation, aspect, and the prevailing wind direction. The topography causes greater rainfall on the eastern, mountainous, windward side (an average of 4000 mm yr^{-1}), while the southern, leeward side is drier (an average of 700 mm yr^{-1}) (Garcia-Martino et al., 1996; Mote et al., 2017; Hosannah et al., 2019). Seasonal variation in precipitation also affects runoff, which is greater in Puerto Rico during the April-November rainy seasons. There is less flow during the dry season (December–March), except in larger streams that originate in igneous and volcanic rocks of the interior (Miller et al., 1997). Most precipitation in Puerto Rico is lost to the atmosphere by evapotranspiration due to the high average temperature, but some water is stored within eleven surface-water reservoirs that are used for hydroelectric power generation and irrigation (Miller et al., 1997).

Dieter et al. (2018) provide estimates of 2015 daily water withdrawals from surface water and groundwater sources as a function of the water-use category. They presented the total water withdrawals by source together with the total population (thousands) to show the most used source and type of water. The population is primarily served by public water utilities, with agricultural irrigation withdrawing more surface and groundwater than all other users (Dieter et al., 2018; Table 3A. 4A).

Approximately 22% of all freshwater needs are met by groundwater withdrawals (Dieter et al., 2018) from three important aquifer systems: Alluvial Valley Aquifers, the South Coast Aquifer, and the North Coast Limestone Aquifer. These aquifers provide critical water sources during high water-demand periods (Miller et al., 1997, Figures 67, 74). The 3- to 8-km wide and 70-km-long South Coast Aquifer is the primary aquifer in southern Puerto Rico (Mendez-Tejeda et al., 2016), while the North Coast Limestone Aquifer is the most extensive and productive freshwater aquifer on the island (Lugo et al., 2001; Maihemuti et al., 2015). Although the quality of water in the aquifers is normally appropriate for most uses, both the North Coast Limestone Aquifer and the South Coast Aquifer have been compromised by saltwater intrusion (Miller et al., 1997; Xu, 2016). Also, these aquifers depend on direct rainfall for recharge, which makes them vulnerable to water stress due to the high population density, industry, tourism, and irrigated agriculture, all placing increasing demands on limited water resources (Mendez-Tejeda et al., 2016).

2.2. The soil-water-balance model version 2.0 (SWB2)

This work includes an estimation of the water-budget components and water availability (measured as net infiltration) to assess the role of Puerto Rico's physical geography (e.g., topography, soils, climate) on the island's water resources. We used the SWB2 model developed by Westenbroek et al. (2018) to accomplish this objective. The model was originally developed for application to the tropical oceanic island of Maui, Hawai'i, in the Central Pacific Ocean, but it has been successfully applied to other oceanic tropical islands since its release (Brewington et al., 2019; Day, 2019; Harlow and Hagedorn, 2018). SWB2 is an updated version of SWB, which includes an option for additional input data to estimate irrigation amounts, as well as capabilities to allow the use of grids with different spatial extents and projections to be combined without requiring resampling and resizing of the grids.

Unlike watersheds in the USA, oceanic islands in tropical climates typically lack detailed, daily, and historical onsite meteorologic, hydrologic, geologic, edaphic (soils), and vegetation information. Thus, SWB2 was selected because it requires commonly available tabular and gridded data types, including temperature, precipitation, land-use classification, hydrologic soil group, flow direction, and soil-water capacity (Westenbroek et al., 2018). Another consideration was the model's prior application to an oceanic tropical island in the Pacific, which is similar to Puerto Rico in terms of climatic and topographic characteristics. Moreover, the Caribbean and Pacific Islands share vulnerabilities related to their isolation, dependence on imports, and dependence on local sources of freshwater, which

make them vulnerable to drought. They are also uniquely different from most of the mainland regions for reasons including, but not limited to, saltwater intrusion and sea-level rise threatening their coastal aquifers (Gould et al., 2018). Even the previous versions of SWB were applied recently in other regions of the U.S. and small tropical islands successfully (Brewington et al., 2019; Day, 2019; Harlow and Hagedorn, 2018).

It is also important to highlight that this study aims to analyze the role of Puerto Rico's physical geography on its water balance island-wise, which makes SWB2 also a better fit when compared to other open-source water budget models, such as Soil and Water Assessment Tool (SWAT) model. SWAT is a basin-scale model and is considered an effective tool for simulating hydrologic processes and water quantity assessments based on watershed specifics (Gassman et al., 2007), which is not the focus of this study. Moreover, the open-source, user-friendly characteristic of SWB2 and the possibility to employ a high-resolution (300-m) analysis of water budget components are other reasons why SWB2 is a better fit than, for example, the GOES-PRWEB model (Harmsen et al., 2021), which uses a

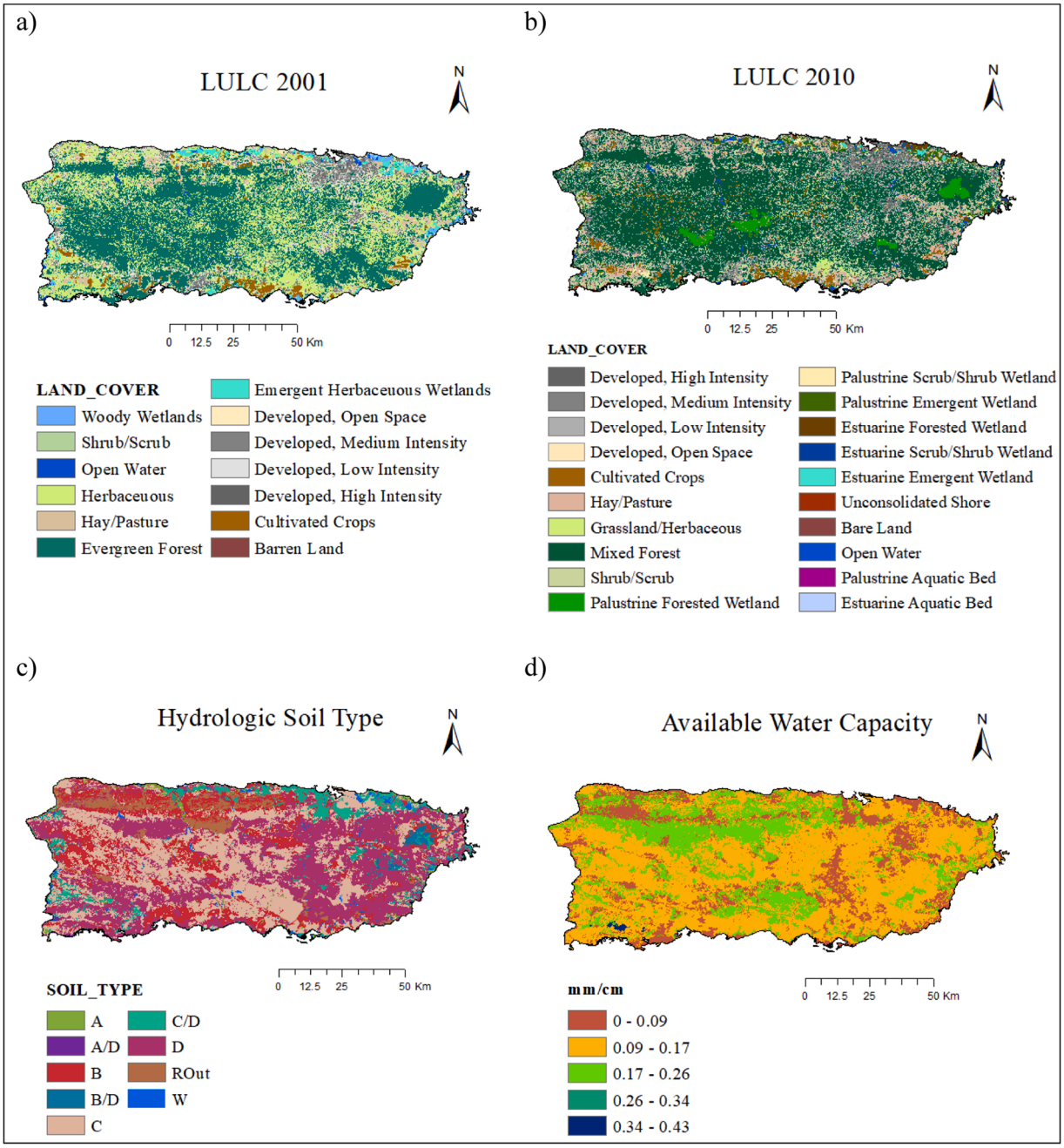

Fig. 2. Spatial inputs for Puerto Rico water budget model showing (a) 2001 land use and land cover, (b) 2010 land use and land cover, (c) hydrologic soil groups, and (d) available soil water capacity (averaged over the first 100 cm of soil depth).

coarser, 1-km resolution water and energy balance model (Harmsen et al., 2021). SWB2 is also superior to SWAT modeling, which lumps landscape features into watershed-scale parameters. However, GOES-PRWEB has been validated and used extensively in Puerto Rico, so it is used here for comparison with SWB2 to evaluate model predictions.

The SWB2 model estimates *net infiltration* instead of groundwater recharge. While not estimating groundwater recharge directly, SWB2 models net infiltration as a proxy. Net infiltration corresponds to deep percolation, which is the downward water flux in the unsaturated zone below the root zone. The difference between net infiltration and recharge is the lag time required for water to move vertically through the unsaturated zone to the water table (Healy, 2010; Westenbroek et al., 2018). There is also a time lag between aquifer recharge and discharge to local streams, which is a function of hydrogeologic conditions. Thus, we follow the SWB2 modeling terminology and use net infiltration to refer to potential groundwater recharge.

The SWB2 model uses a modified Thornthwaite and Mather (1957) soil-moisture accounting method to calculate net infiltration at a daily frequency on a grid-by-grid cell basis. It uses sources and sinks of water within each grid cell based on input climate data and landscape characteristics. While running the model, soil moisture is updated every day as the difference between these sources and sinks, and net infiltration is only computed when soil moisture exceeds the field capacity, otherwise it is zero.

Eq. 1 summarizes the water-budget components used in this study and explains how SWB2 quantifies net infiltration, *NI*, which is defined as the deep percolation (i.e., soil percolation below the root zone that eventually becomes groundwater recharge):

$$NI = R - I - Roff - AET - \Delta S \quad (1)$$

where R is gross precipitation, I is interception, *Roff* is runoff, *AET* is actual evapotranspiration, and ΔS is change in soil moisture. Both I and ΔS are considered storage components within the SWB2 model. Model outputs are reported in English units (inches) but are converted to SI units here. The SWB2 model grid cell resolution was defined as 300 m for this study.

This study used the following input datasets for the SWB2 model: daily gridded climate data from Daymet (Version 3) at 1-km resolution (precipitation, maximum temperature, and minimum temperature) from 1980 to 2019; hydrologic soil types, and available water soil capacity (AWC, 0–1-m depth) from Gridded Soil Survey Geographic (gSSURGO) database at 10-m resolution (USDA, 2020); and two land use and land cover (LULC) datasets at 30-m resolution. The 2001 LULC dataset is from the National Land Cover Database, and the 2010 LULC dataset is from NOAA Office for Coastal Management (NOAA/OCM). All the non-transient SWB2 input data are shown in Fig. 2. Note that Daymet Version 3 was used instead of Version 4 because preliminary analysis indicates that Version 3 performs better in Puerto Rico when compared to observed runoff (Jazlynn Hall, Columbia University, pers. comm.).

The SWB2 model requires that gross precipitation (R) exceeds the assigned interception (I) before net precipitation reaches the ground (Harlow and Hagedorn, 2018; Westenbroek et al., 2018). Thus, we determined interception amounts for the different LULC types based on previous studies (Harlow and Hagedorn, 2018). We defined the growing season as the period corresponding to the April–November rainy seasons in Puerto Rico, while the dry season (December-March) is the non-growing season (Table 1).

The model estimates direct runoff (*Roff*) using the curve number method for the different LULC classes and hydrologic soil groups. We assigned curve numbers based on published values (Huffman et al., 2011; Kent, 1973; Westenbroek et al., 2018), presented in Table 2. Group A, B, C, D, A/D, B/D, and C/D soils are originally from the gSSURGO dataset (USDA, 2020), while the group W and ROut soils correspond to *water* and *rock outcrop* categories created by the authors to account for gaps within the gSSURGO dataset. We assign group W soils to all water and wetland landscapes (e.g., riverwash, alluvial land, and open water) and assign group ROut soils to

Table 1
Puerto Rico interception values (mm day-1) for growing (rainy) and non-growing (dry) seasons based on land use and land cover (LULC) used as input in the Soil Water Balance Model 2 (SWB2). The rainy season extends from April to November, and dry season from December to March.

Land Use – Land Cover	Season	
	Rainy	Dry
High Intensity Developed	0.00	0.00
Medium Intensity Developed	0.51	0.25
Low Intensity Developed	0.51	0.25
Developed, Open Space	0.00	0.00
Cultivated Crops	3.81	3.81
Pasture/Hay	2.03	0.76
Grassland/Herbaceous	2.03	0.76
Mixed Forest	5.08	5.08
Shrub/Scrub	3.81	3.81
Palustrine Forested Wetland	5.08	5.08
Palustrine Scrub/Shrub Wetland	3.81	3.81
Palustrine Emergent Wetland	0.51	0.25
Estuarine Forested Wetland	5.08	5.08
Estuarine Scrub/Shrub Wetland	3.81	3.81
Estuarine Emergent Wetland	0.51	0.25
Unconsolidated Shore	0.00	0.00
Bare Land	0.00	0.00
Open Water	0.00	0.00
Palustrine Aquatic Bed	0.00	0.00
Estuarine Aquatic Bed	0.00	0.00

Table 2
Relationship between hydrologic soil groups and Land Use and Land Cover (LULC) Curve Numbers and maximum net infiltration (mm d^{-1}) used as input in the Soil Water Balance Model 2 (SWB2).

LULC Curve Numbers	Hydrologic Soil Group								
	A	B	C	D	W	ROut	A/D	B/D	C/D
High Intensity Developed	89	92	94	95	70	95	93	94	95
Medium Intensity Developed	77	85	90	92	70	95	85	87	91
Low Intensity Developed	67	78	85	89	70	95	79	84	87
Developed, Open Space	49	69	79	84	70	95	65	75	82
Cultivated Crops	39	61	74	80	70	95	62	71	77
Pasture/Hay	39	61	74	80	70	95	62	71	78
Grassland/Herbaceous	39	61	74	80	70	95	62	71	77
Mixed Forest	30	55	70	77	70	95	56	65	74
Shrub/Scrub	35	56	70	77	70	95	59	65	74
Palustrine Forested Wetland	30	55	70	77	70	95	56	65	74
Palustrine Scrub/Shrub Wetland	35	56	70	77	70	95	59	65	74
Palustrine Emergent Wetland	30	58	71	78	70	95	56	68	74
Estuarine Forested Wetland	30	55	70	77	70	95	56	65	74
Estuarine Scrub/Shrub Wetland	35	56	70	77	70	95	59	65	74
Estuarine Emergent Wetland	30	58	71	78	70	95	56	68	74
Unconsolidated Shore	70	70	70	70	70	70	70	70	70
Bare Land	74	83	88	90	70	95	82	85	89
Open Water	70	70	70	70	70	95	70	70	70
Palustrine Aquatic Bed	70	70	70	70	70	95	70	70	70
Estuarine Aquatic Bed	70	70	70	70	70	95	70	70	70
Maximum Net Infiltration	101.6	15.24	6.10	3.05	0.76	0.25	101.6	3.05	3.05

all rock outcrops and rocky lands. We assign group C soils to grid cells with no data available, which corresponds to the main soil type in the region (i.e., silty clay loam) according to local experts (Eric Harmssen, University of Puerto Rico-Mayagüez, pers. comm.). We assign group C/D soils to urban lands due to their lower permeability.

SWB2 avoids the overestimation of net infiltration by allowing the user to assign maximum infiltration rates that specify the maximum amount of daily recharge for each hydrologic soil type (Table 2). After reaching the maximum daily net infiltration, the remaining water is classified as rejected net infiltration and is diverted to surface water. Therefore, the total runoff (*Roff*) is the sum of the direct runoff and the rejected net infiltration. In this study, we use the same maximum infiltration rates used by Westenbroek et al. (2018).

Additionally, three potential evapotranspiration (PET) estimation methods are available in the SWB2 model. We employed the Hargreaves-Samani method (Hargreaves and Samani, 1985), which is considered a simplified version of the FAO Penman-Monteith method that is not included in the model. The Hargreaves-Samani method requires spatially distributed minimum and maximum daily temperatures, which we obtained from Daymet (Version 3). Then, SWB2 estimates actual ET (AET) as a function of PET, net precipitation, and the current soil moisture within each grid cell. The model assumes that AET equals PET whenever net precipitation exceeds PET. Otherwise, AET is equal to the amount of water that can be extracted from the soil via AET considering the computed values of soil moisture retention tables of Thornthwaite and Mather (1957) and modified by Westenbroek et al. (2010). The Thornthwaite-Mather function requires estimates of the maximum soil moisture storage capacity, which was determined using AWC data from gSSURGO multiplied by the rooting depth within each hydrologic soil type, which was defined using Westenbroek et al. (2018) (Table S1 in Supplementary Material).

Finally, the SWB2 model requires an initial amount of soil moisture to calculate potential soil saturation and net infiltration (or evapotranspiration) on Day 1, which was determined using the reference value provided by Westenbroek et al. (2018) for the SWB2 model in Maui, Hawai'i. Additionally, we also ran the SWB2 model for a one-year warm-up period prior to the analysis period to account for initial transients. A detailed control file including all the parameters used to run the SWB2 model for Puerto Rico is provided in Supplementary Material (Table S2).

2.3. Data periods

Two periods were selected for modeling, a baseline period (1981–2010) and a recent decade (2010–2019). This data bifurcation created a climatology reference period (baseline) that is used to evaluate whether changes are occurring in the latter period. To account for possible differences in LULC in Puerto Rico, we ran the baseline climatology using LULC from 2001 and the recent decade with an updated LULC from 2010, with differences shown in Fig. 2.

After defining the baseline climatology (1981–2010) and the recent decade (2010–2019) to run the SWB2 model, we identified four drought years (10% of the period of analysis) based on the lowest annual average rainfall amounts in Puerto Rico: 1994, 1997, 1991, and 2015 (in descending order). Then, we averaged SWB2 outputs from these years to create drought years' water budget annual maps. This allowed us to compare the spatial distribution of net infiltration over Puerto Rico during the baseline climatology (1981–2010) with drought years to determine regions with greater water scarcity.

2.4. Model evaluation

Our goal was to test a model that requires no calibration, which is dependent on input parameters that accurately represent field conditions and do not require modification. We employ this strategy because many oceanic islands in tropical climates lack field data for model calibration. Developing field datasets in these settings is laborious, expensive, and requires long-term commitments.

We know that multiple methods are used to assess water-budget models based on the availability of data. In this study, we assessed the SWB2 outputs in two ways: 1) by comparing SWB2 against the GOES-PRWEB (Mecikalski and Harmsen, 2019; Harmsen et al., 2021), which is an existing water-budget model for Puerto Rico, and 2) by comparing SWB2 to observed watershed streamflow from US Geological Survey (USGS) stream gauges.

Fig. 3 compares SWB2 with GOES-PRWEB model outputs for the decade of overlapping data (i.e., 2009–2019). Rainfall and runoff comparisons (Fig. 3**a,d**) both demonstrated a positive correlation between SWB2 and GOES_PRWEB models of + 0.6 and + 0.5, respectively. However, only rainfall correlation was statistically significant ($p = 0.10$), while the relationship between runoff was not statistically significant. From 2009–2014, the rainfall input from SWB2 presented at least 30% more annual average rainfall than the GOES-PRWEB model. Although further investigation is needed to assess which rainfall input data is more accurate (Daymet Version 3 used in SWB2, or NOAA's Advanced Hydrologic Prediction Service (AHPS) used in GOES_PRWEB), both models' rainfall amounts from 2015 to 2019 are in good agreement, which includes at least two extreme events: the intense drought of 2015 and hurricanes Irma and Maria in 2017. The models' correlation for AET was + 0.5, which is statistically significant ($p = 0.10$), although SWB2 seemed to overestimate AET when compared to GOES_PRWEB.

Finally, the correlation between the SWB2 and GOES_PRWEB net infiltration was very strong (+0.8) and statistically significant ($p = 0.01$). Therefore, considering that the models used different approaches to estimate the water budget as well as different input data sources, the statistically significant correlation, together with the similarities among models' results of annual net infiltration, suggest that they should both be considered suitable options for estimating net infiltration in Puerto Rico.

We also analyzed the SWB2 model performance in comparison with observed streamflow data from the USGS. The watersheds selection in Puerto Rico was based on their spatial distribution over the island and the availability of data that overlapped the most with our period of study (1981–2019). The following watersheds were included in this study (from larger to smaller): Manati (330.7 km^2), Guanajibo (310.5 km^2), Cibuco (226.8 km^2), Fajardo (38.3 km^2), and Espiritu Santo (22.5 km^2) (Fig. 4).

From the SWB2 model, we used *Roff* (runoff + rejected net infiltration) and converted the model outputs to streamflow ($m^3\ s^{-1}$) to create the simulated data and compare it with the observation. In the observation data, we performed baseflow separation through the Web-based Hydrograph Analysis Tool (WHAT) system, which used the Eckhardt filter method and was tested to provide more

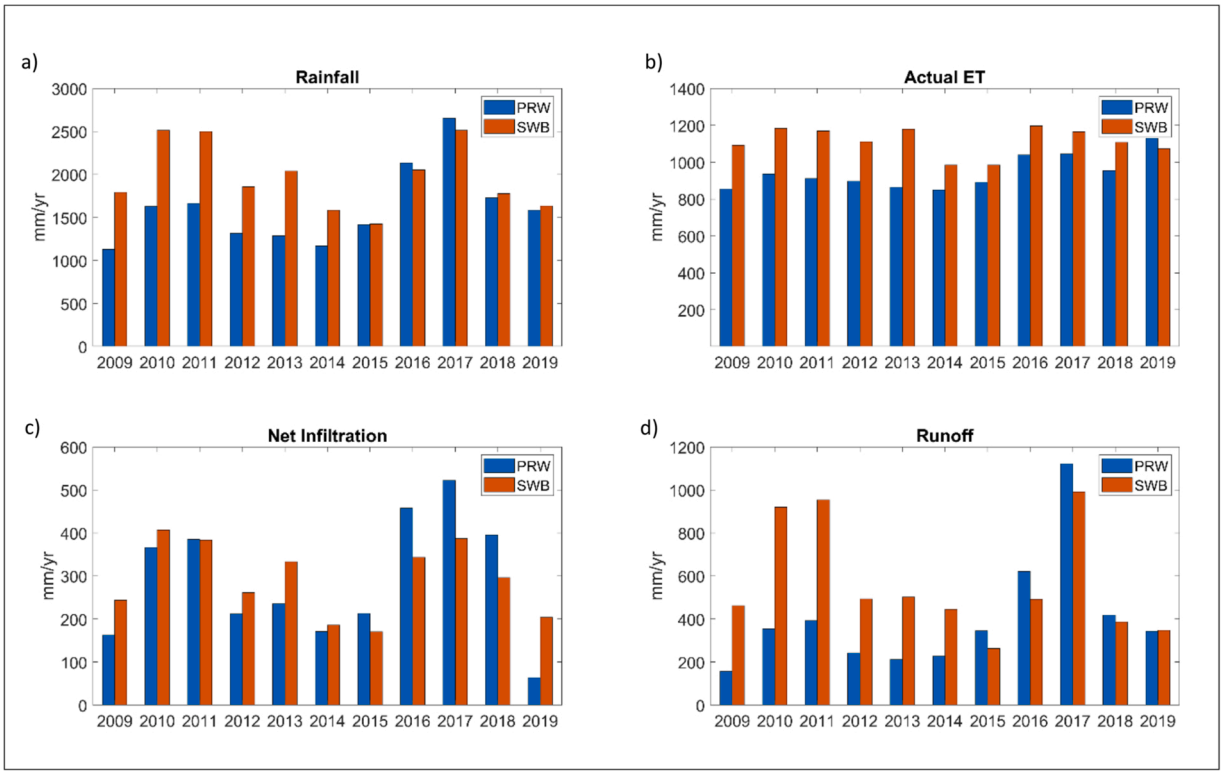

Fig. 3. Comparison of predicted annual totals (mm yr^{-1}) between SWB2 (orange) and GOES-PRWEB (blue) for (a) actual evapotranspiration (ET), (b) net infiltration, (c) rainfall, and (d) runoff, from 2009 to 2019.

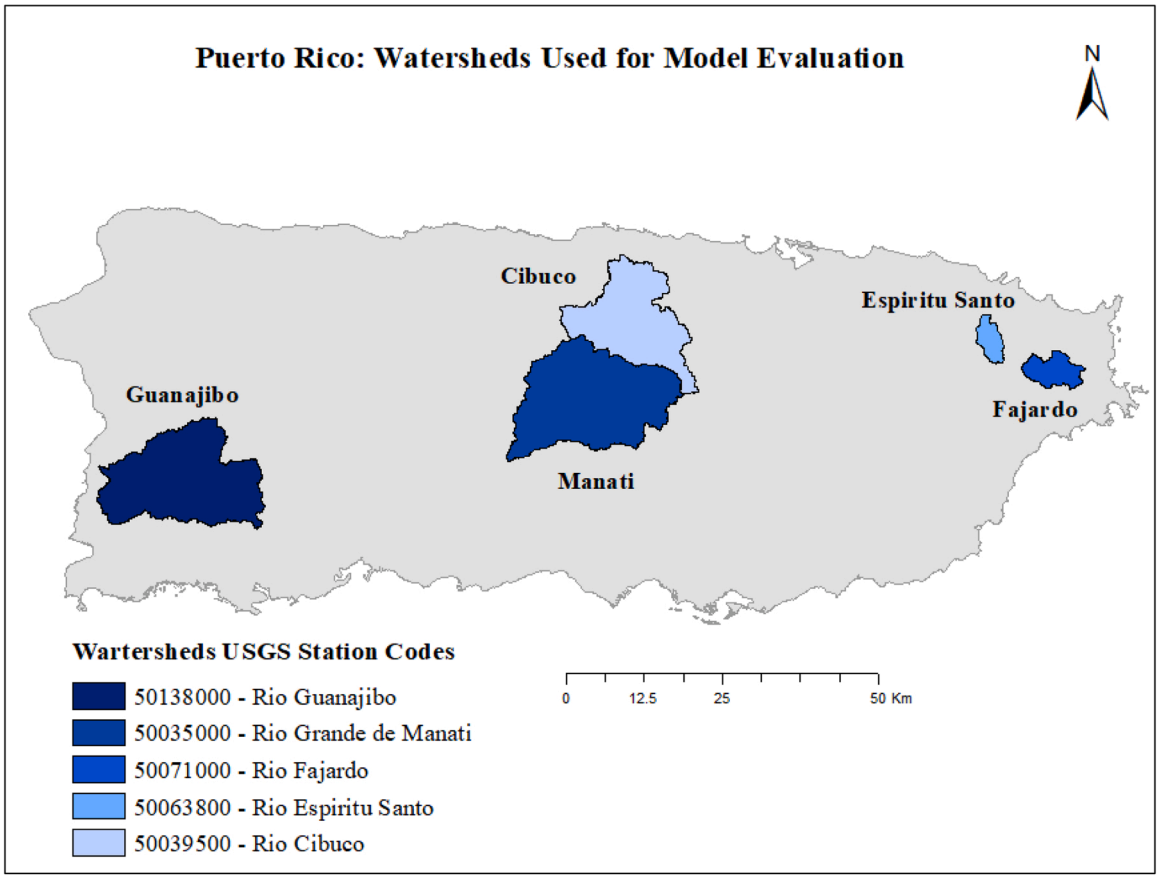

Fig. 4. Puerto-Rican watersheds selected from the U.S. Geological Survey for SWB2 model evaluation; Manati (330.7 km^2), Guanajibo (310.5 km^2), Cibuco (226.8 km^2), Fajardo (38.3 km^2), and Espiritu Santo (22.5 km^2).

consistent results than a manual separation of baseflow (Lim et al., 2005). We selected the parameter "perennial streams with hard rock aquifers" for all watersheds analyzed because they are all located in the mountainous area of the island.

Finally, we compared the simulated versus observed direct runoff by running three model performance statistical tests commonly used in previous studies (Ang and Oeurng, 2018; Kumar et al., 2017; Moriasi et al., 2007), which are the Nash-Sutcliffe efficiency (NSE), the RMSE-observations standard deviation ratio (RSR), and the percent bias (PBIAS). We perform the statistical tests separately for each period of analysis because we have used different LULC to run the SWB2. The definition of each model performance test is summarized below, with additional details available in Moriasi et al. (2007):

- NSE indicates how well the plot of observed versus simulated data fits the 1:1 line by a normalized statistic that determines the relative magnitude of the residual variance ("noise") compared to the measured data variance ("information"). NSE ranges from $-\infty$ and 1.0 (1 inclusive), where 1.0 is the optimal value. Values between 0.0 and 1.0 are viewed as acceptable levels of performance.
- RSR standardizes the RMSE, which is one of the commonly used error index statistics, using the observations standard deviation. RSR is calculated as the ratio of the RMSE and standard deviation of measured data. It varies from the optimal value of 0, which indicates zero residual variation and perfect model simulation, to a large positive value. Therefore, the lower the RSR the better the model simulation.
- PBIAS measures the average tendency of the simulated data to be larger or smaller than the observed data. The optimal value is 0.0, with low-magnitude values indicating accurate model simulation. Positive values mean model underestimation bias, and negative values mean model overestimation bias.

The timeseries presented in Figs. S1 and S2 provide a comparison of the monthly average simulated versus observed direct runoff for Puerto Rico during the baseline climatology and recent decade, respectively. Overall, the model was consistent in predicting peak flows over time, mainly in the larger area watersheds, while it underestimated most of the low flows. In the small watersheds located in the Luquillo Mountains, such as Fajardo and Espiritu Santo, the model slightly underestimated the flow over time. These poor predictions of lower flows are likely due to the lack of consideration of aquifer hydraulic behavior in the SWB2 model.

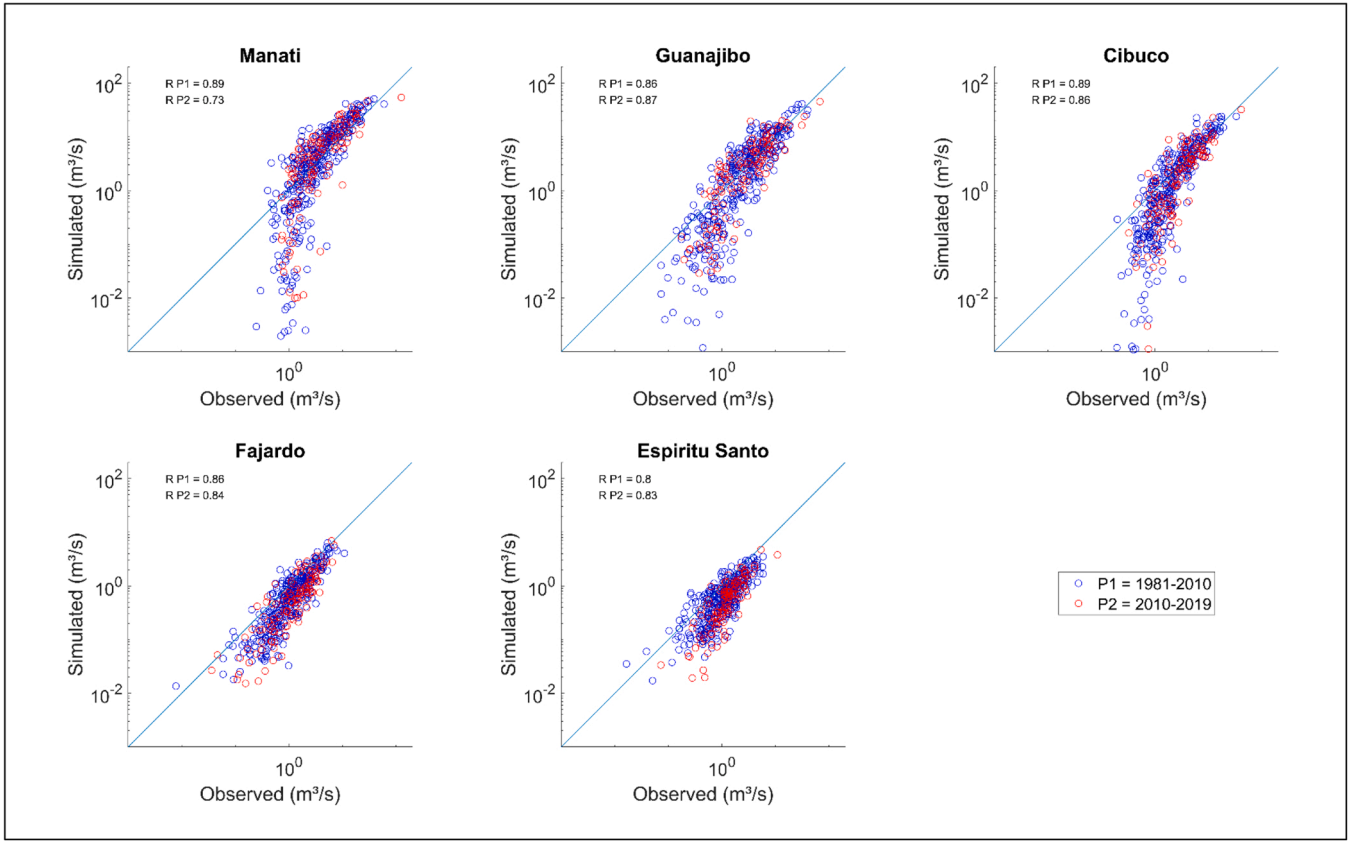

Fig. 5. Comparison of Puerto-Rican SWB2-predicted runoff (y-axis) versus USGS-observed runoff (x-axis). Blue dots indicate baseline climatology (1981–2010), and red dots indicate the recent decade (2010–2019). R-values are correlation coefficients between simulated and observed data.

Fig. 5 shows both scenarios together and reinforces that the model better simulated average and peak flows (mainly for Manati, Cibuco, Guanajibo), but underestimated low flows, while for Fajardo and Espiritu Santo basins, the model is overall underestimating the flow. However, the relationship between the simulated and observed data is very strong and statistically significant ($p = 0.01$) for all watersheds, with a correlation coefficient $\geq +0.8$, except for Manati in the recent decade, which presented a correlation coefficient of + 0.7.

Moreover, the model performance statistics for Puerto Rico for the baseline climatology (Table 3) indicated that the best simulation occurred in Guanajibo with both NSE (0.75) and RSR (0.50) rating as good model performance, while its PBIAS indicates the model has a very good performance with an overestimation of only 2.9% of the flow. Cibuco came next, with a similar model performance indicating a good rate for NSE (0.71) and RSR (0.54) and very good for PBIAS (+8.2%), while the simulation of direct runoff for Manati was satisfactory in all model performance statistics (NSE = 0.52, RSR = 0.69, PBIAS = −23.5%). For smaller basins, SWB2 was very close to satisfactory for Fajardo's NSE (0.45) and RSR (0.74) but it did not have a satisfactory performance for Espiritu Santo.

In the recent decade, on the other hand, the SWB2 performed slightly better for Fajardo and Espiritu Santo but slightly worse for Manati, Cibuco, and Guanajibo. In fact, the Fajardo simulation in the recent decade had a satisfactory NSE (0.60) and RSR (0.63), with a PBIAS indicating the model underestimated only 34% of the flow (Table 3). For Guanajibo and Cibuco, the model performed very similarly and kept a good NSE and RSR, and very good PBIAS, while Manati was slightly below the satisfactory performance. Overall, Espiritu Santo was the watershed simulation with the worst performance when comparing all the statistical tests and periods, which was expected as the smaller watershed analyzed here.

The slightly better performance of the model in the larger watersheds during the baseline climatology (1981–2010) than in the recent decade (2010–2019) may be related to the fact that the Caribbean, in general, has been presenting a negative trend in drought index indicating more frequent and severe drought events (Herrera and Ault, 2017; Herrera et al., 2018; Moraes et al., 2022). Because the model did not well-reproduce low flows in Puerto Rico, we hypothesize that the increase in the occurrence and intensity of drought events may have affected the overall model performance in the recent decade, together with the fact that there is a lack of consideration of aquifer hydraulic behavior in the SWB2 model. Therefore, this limitation of the model should be taken into consideration when analyzing the results from the drought years, particularly because they are linked to low flows.

On the other hand, the observed improvement in SWB2 performance during the recent decade in smaller watersheds located within the Luquillo Mountains could be related to the increase in data availability and equipment recently installed by the Long-Term Ecological Research (LTER) project within the tropical rainforest. This, along with newly available daily rainfall data from an updated version of Global Historical Climate Network (Thornton et al., 2016), has probably improved model performance in Fajardo and Espiritu Santo. However, we believe that the accuracy of the Daymet rainfall data and its spatial resolution of 1 km may have a larger effect in smaller watersheds, like Espiritu Santo, when compared to the larger basins. This basin contains fewer than 22 grid cells of rainfall data, a coarse resolution for the accuracy and analysis of rainfall needed in the steeply slope terrain located in the Luquillo Mountains.

Moreover, the basins where the model performed better (e.g., Manati, Cibuco, Guanajibo, Fajardo) all have a large portion of group C soils (e.g., silty clay loam), which is the most common soil type in Puerto Rico. This may indicate that the SWB2 model performs satisfactorily for most of the areas on the island. Although we recommend caution interpreting the results of the SWB2 model mainly for areas located in the steep slope of the Luquillo Mountains, where the model is mostly underestimating streamflow, we believe the model has performed well in Puerto Rico without the need for calibration, and it should be considered as an option for future studies interested in water budget modeling on this and other oceanic islands with tropical climates.

3. Results

3.1. Baseline climatology versus recent decade

Annual net infiltration in Puerto Rico had a similar spatial distribution when comparing the baseline climatology (1981–2010) and

Table 3
Evaluation of SWB2 model performance for Puerto Rico during two periods: the baseline climatology (1981–2010) and the recent decade (2010–2019). The performance rates are highlighted as follows: satisfactory performance is in yellow, good performance is in green, and very good performance is in blue, all according Moriasi et al. (2007). Gray values are almost satisfactory performance.

Watershed	Area	Baseline Climatology			Recent Decade		
	(km^2)	PBIAS	NSE	RSR	PBIAS	NSE	RSR
Manati	330.7	-23.5%	0.52	0.69	-39.9%	0.35	0.81
Guanajibo	310.5	2.9%	0.75	0.50	-8.8%	0.66	0.58
Cibuco	226.8	8.2%	0.71	0.54	-0.6%	0.69	0.56
Fajardo	38.3	43.5%	0.45	0.74	34.0%	0.60	0.63
Espiritu Santo	22.5	50.3%	0.28	0.85	40.7%	0.34	0.81

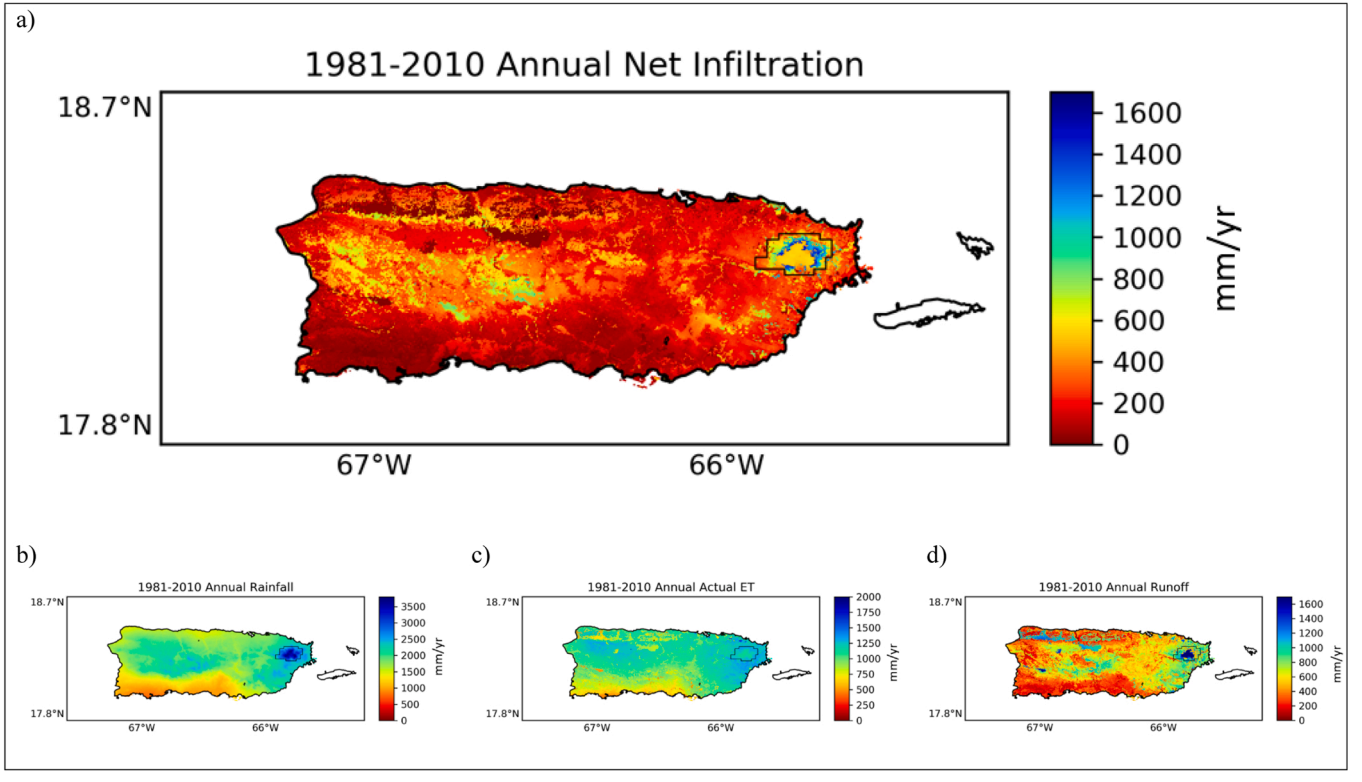

Fig. 6. Annual water-budget components during the baseline climatology (1981–2010): (a) net infiltration, (b) rainfall (gross precipitation), (c) actual ET, and (d) runoff. Black contour in northeastern Puerto Rico indicates El Yunque National Forest in the Luquillo Mountains.

the recent decade (2010–2019). Figs. 6(a) and 7(a) show that the estimated net infiltration was greater in the central-west and northern portion of the island ranging from 600 to 900 mm yr^{-1} (baseline) to 700–1000 mm yr^{-1} (recent decade). The greatest net infiltration occurred in eastern Puerto Rico, in lower elevations of the Luquillo Mountains/El Yunque National Forest, where it reached values greater than 1500 mm yr^{-1} during both periods of analysis. When examining the other water budget elements, we see that central and eastern Puerto Rico were areas with greater values of AET and runoff, when compared to other areas within the island, but they were also the areas with the greatest annual rainfall ($\geq$ 2500 mm yr^{-1}). Therefore, the abundant rainfall in those areas provided extra water available for net infiltration. Another characteristic of the areas with greater net infiltration in Puerto Rico is that they are in the heavily vegetated mountainous areas of the island (i.e., Cordillera Central and Luquillo Mountains) and have soil types B and C with greater infiltration rates (Fig. 2**c**). Southern Puerto Rico, on the other side, was where the lowest amount of net infiltration occurred in both periods. That region is known for its dry climate, and we can see that while the annual rainfall was $\leq$ 1000 mm yr^{-1}, the annual AET was as high as in the rest of the island ($\sim$ 750 mm yr^{-1}), which contributed to its lower annual net infiltration ($\leq$ 200 mm yr^{-1}).

While water-budget components are geographically similar between periods, there are some important differences in the amount of water distributed across the island, which can be evaluated by taking the difference between the recent decade minus the baseline climatology (Fig. 8). In central and western areas, net infiltration was at least 250 mm yr^{-1} greater in the recent decade than in the baseline climatology, while AET was similar, and runoff increased in the recent decade ($\geq$ 100 mm yr^{-1}). The increased rainfall on most of the island could explain these differences, with the central-west region receiving at least 400 mm yr^{-1} more rainfall in the recent decade than during the baseline climatology. Yet, the opposite occurred in the Luquillo Mountains, where less rainfall was registered from 2010 to 2019 (≤ -250 mm yr^{-1}), along with less runoff (≤ -200 mm yr^{-1}) and less AET (≤ -50 mm yr^{-1}). Consequently, net infiltration decreased in eastern Puerto Rico in the recent decade (≤ -100 mm yr^{-1}).

In addition to the spatial distribution of rainfall, the temporal distribution is also important. The greatest rainfall occurred in the recent decade (Fig. 9), with Hurricanes Irma and Maria in 2017 and other large events in 2010 and 2011. Three of the four years with the lowest rainfall totals (i.e., 1991, 1994, 1997) occurred during the baseline period, while only one (2015) occurred during the recent decade.

Along with rainfall, LULC changes may also affect net infiltration differences between the baseline climatology and the recent decade. In Fig. 2**(a,b)**, we see a reduction in the herbaceous category between 2001 and 2010 LULC, with a concomitant increase in cultivated crops in the central area. Greater rainfall in central Puerto Rico and less herbaceous vegetation to intercept rainfall increases net infiltration. On the other hand, the conversion of herbaceous to developed land in eastern Puerto Rico, together with decreased rainfall, may have contributed to the decrease in net infiltration during the recent decade.

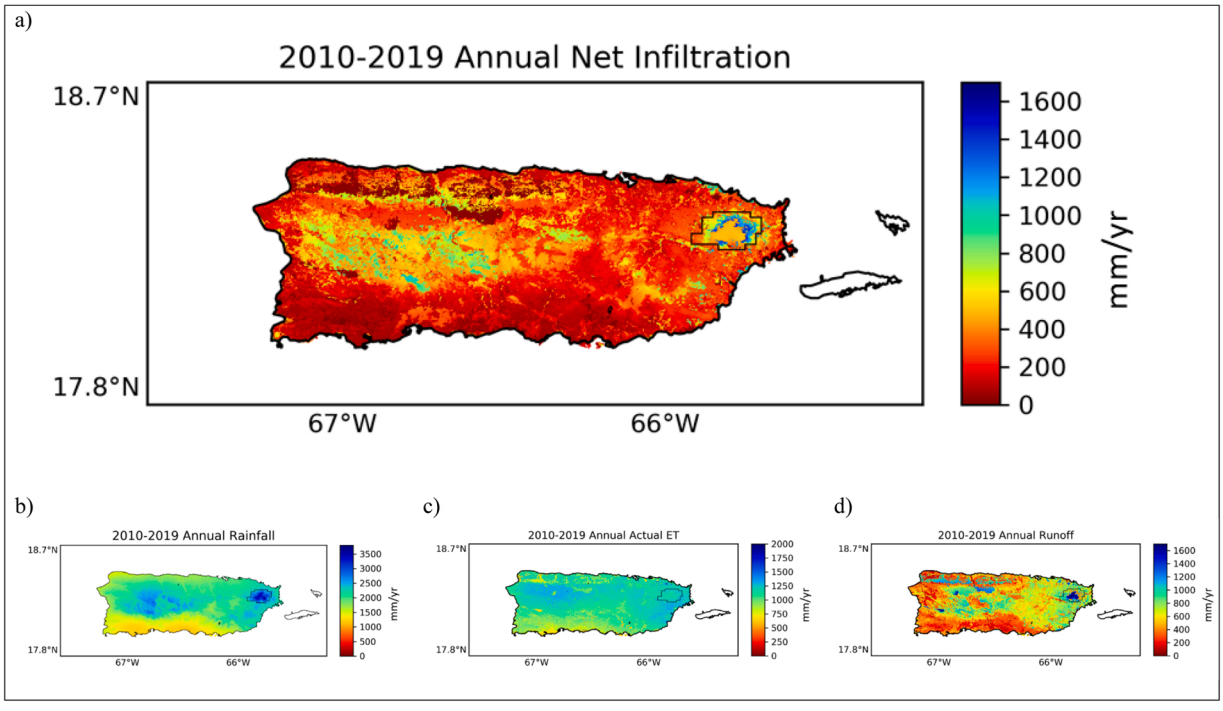

Fig. 7. Annual water-budget components during the recent decade (2010–2019): (a) net infiltration, (b) rainfall (gross precipitation), (c) actual ET, and (d) runoff. Black contour in northeastern Puerto Rico indicates El Yunque National Forest in the Luquillo Mountains.

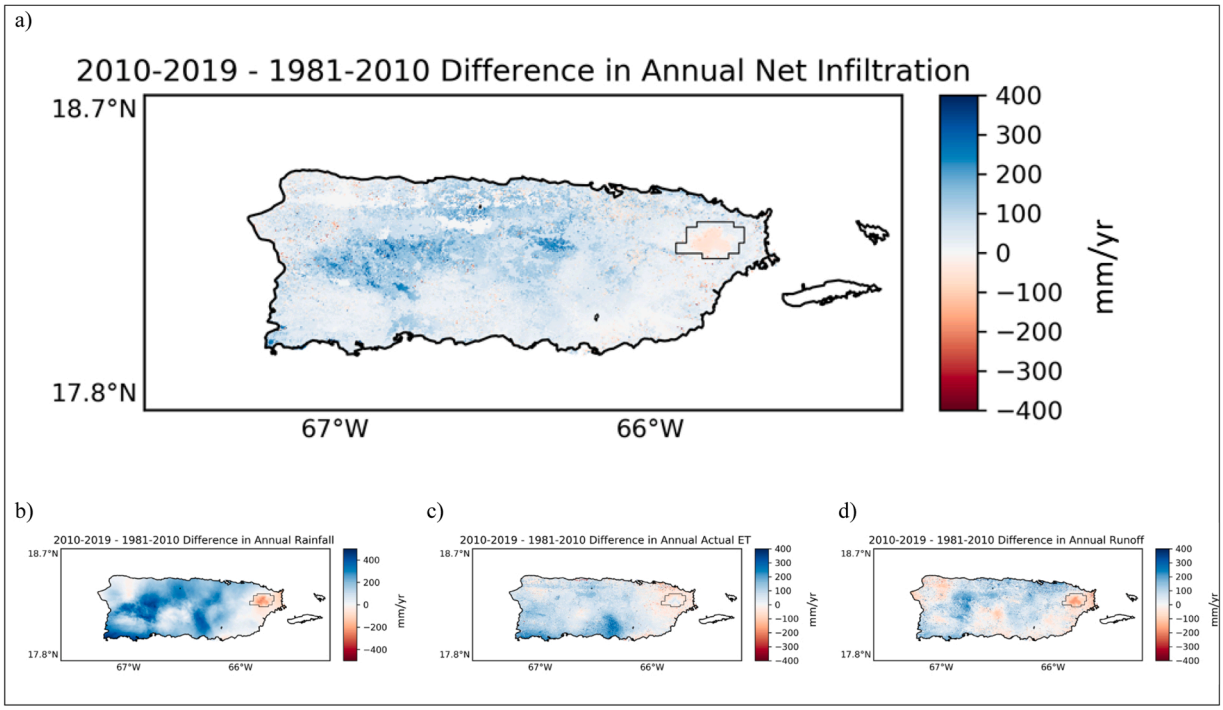

Fig. 8. Difference between recent decade and baseline climatology for water-budget components: (a) net infiltration, (b) rainfall (gross precipitation), (c) actual ET, and (d) runoff. Black contour in northeastern Puerto Rico indicates El Yunque National Forest in the Luquillo Mountains.

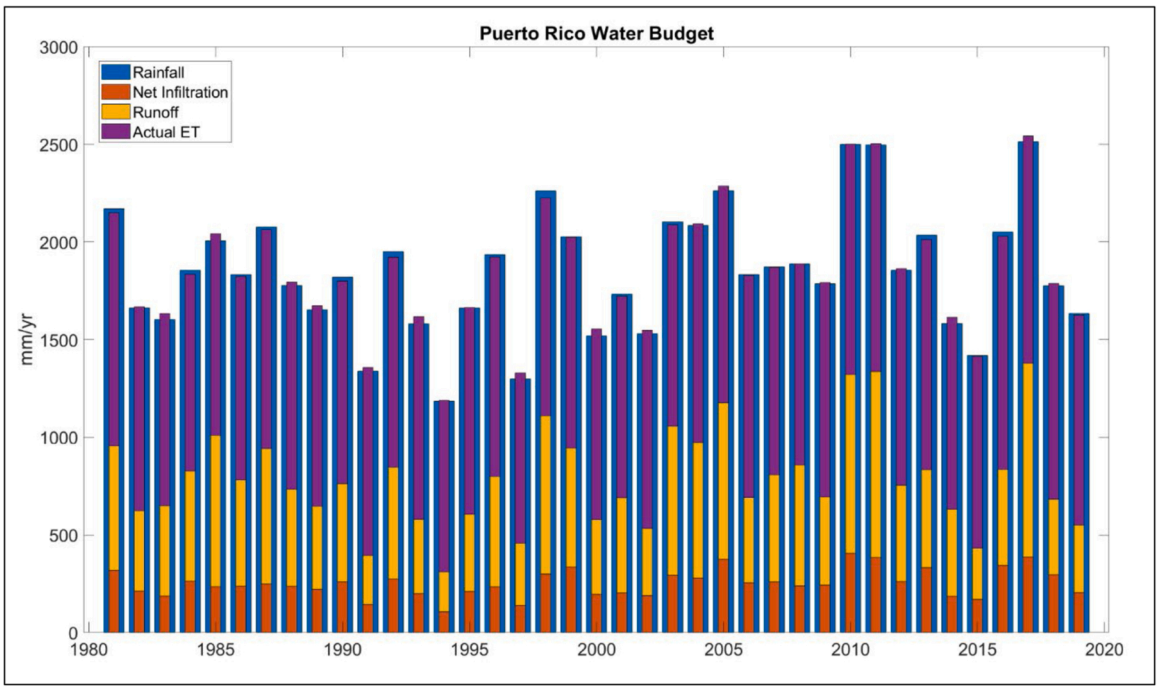

Fig. 9. Annual water-budget components for 1981–2019. Blue bars represent rainfall inputs, colored bars represent water withdrawals, purple is actual ET, yellow is runoff, orange is net infiltration.

3.2. Drought years versus baseline climatology

We selected four years (in descending order: 1994, 1997, 1991, 2015) to represent drought conditions (see Methods section). Fig. 10 shows the annual spatial distribution of the water budget components during those drought years and indicated a much smaller area as well as lower values of net infiltration when compared to the baseline climatology.

During drought years, Puerto Rico had only small areas of net infiltration still occurring in the central-west of the island, with values between 300 and 500 mm yr^{-1}, and in the lower elevations of Luquillo Mountains/El Yunque National Forest ($\leq$ 800 mm yr^{-1}). Most of the island, however, has minimal net infiltration ($\leq$ 200 mm yr^{-1}). Most of southern Puerto Rico receives less than 700 mm yr^{-1} of rainfall, while a similar amount of water was lost through AET (Fig. 10**b,c**), which resulted in little water for net infiltration ($\leq$ 100 mm yr^{-1}). The northern area of Puerto Rico also suffered from lower precipitation and higher AET, resulting in infiltration concentrated in a small area.

Puerto Rico had a reduction in net infiltration of at least 150 mm yr^{-1} during drought years, except for some rock outcrops located in the north of the island, which showed no difference (Fig. 11). However, the areas most affected by drought were parts of central and northern Puerto Rico as well as the Luquillo Mountains, where the reduction in net infiltration was more than 400 mm yr^{-1} below the baseline period. Central and eastern Puerto Rico were areas where the greatest departure in precipitation occurred (≤ -700 mm yr^{-1}), together with a reduction in runoff (≤ -400 mm yr^{-1}). Although AET mostly decreased over the island during drought years, central-west and eastern Puerto Rico registered similar amounts of AET when compared to the baseline climatology.

Together with large reductions in rainfall, higher AET could also explain why central-west and eastern Puerto Rico had the greatest difference in net infiltration during drought years. The difference in net infiltration in southern Puerto Rico was smaller than the rest of the island (≤ -100 mm yr^{-1}) when comparing drought years and the baseline climatology.

4. Discussion

4.1. Baseline climatology versus recent decade

The role of physical geography (e.g., topography, vegetation, climate) on the water cycle is evident when comparing the drier south with the wetter east and central Puerto Rico (Figs. 6 and 7). Southern Puerto Rico is known as a drier region (lower humidity and precipitation, higher PET) and is classified as a "dry forest" (Holdridge, 1967). The lower humidity is related to its geographic location on the leeward side of the Central Mountain Range (i.e., Cordillera Central), which creates a shield blocking the Atlantic moisture and making the south drier than other regions of Puerto Rico (Torres-Valcárcel et al., 2014). Moreover, recent studies confirmed the dryness of this region by showing that the potential evapotranspiration is greater than rainfall from 2009 to 2018, indicating a greater water demand than water supply and resulting in dry soils and low groundwater recharge in southern Puerto Rico (Harmsen, 2019).

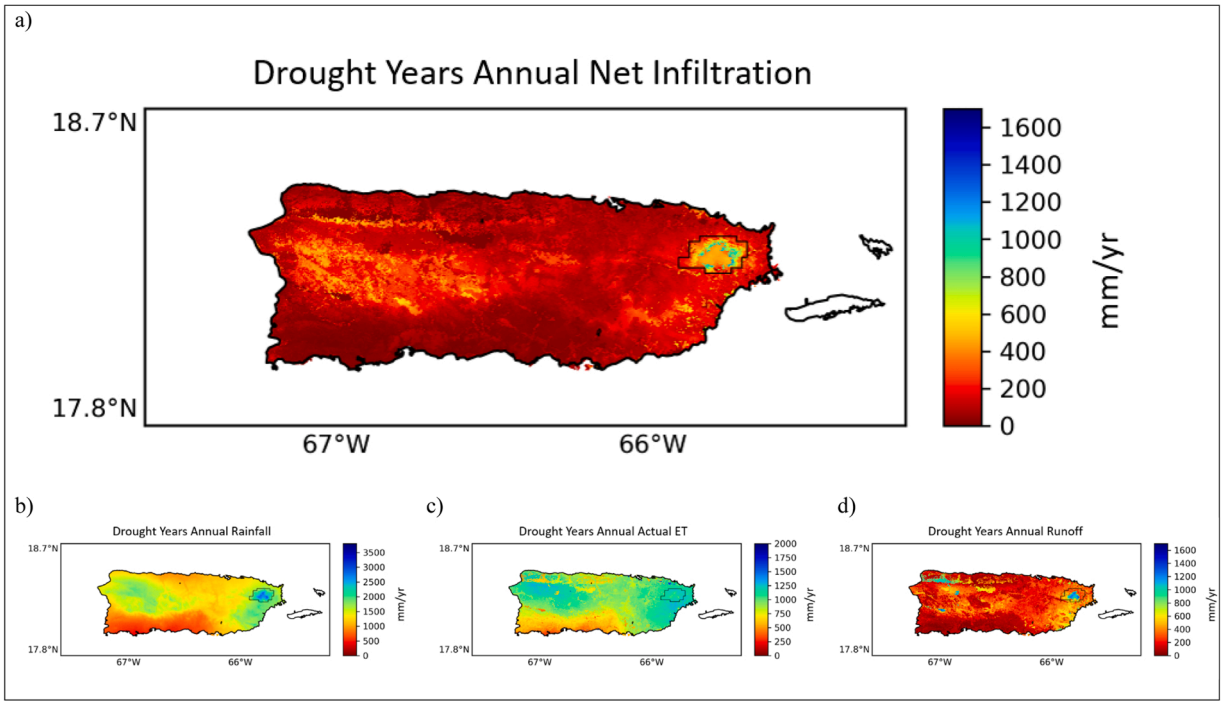

Fig. 10. Annual water-budget components during drought years (1991, 1994, 1997, and 2015): (a) net infiltration, (b) rainfall (gross precipitation), (c) actual ET, and (d) runoff. Black contour in northeastern Puerto Rico indicates El Yunque National Forest in the Luquillo Mountains.

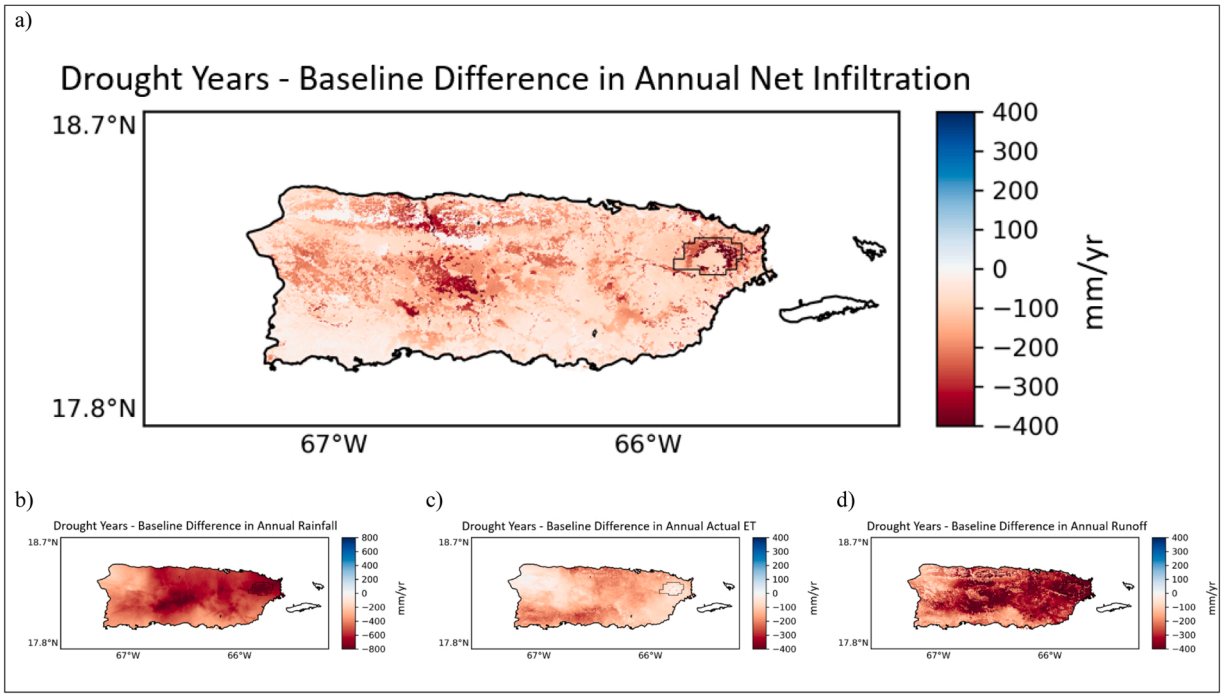

Fig. 11. Difference between drought years and baseline climatology for water-budget components: (a) net infiltration, (b) rainfall (gross precipitation), (c) actual ET, and (d) runoff. Black contour in northeastern Puerto Rico indicates El Yunque National Forest in the Luquillo Mountains.

The presence of group D soils with lower infiltration rates (Fig. 2**c**), could also contributed to lower net infiltration rates in the south.

Orographic uplift of northeasterly winds from the Atlantic Ocean along the Cordillera Central and Luquillo Mountains results in greater rainfall that makes these regions wetter than the rest of the island (Hosannah et al., 2019; Sobel et al., 2011). Additionally, these mountains are covered by evergreen tropical vegetation, with the Luquillo Mountains being the location of the El Yunque National Forest. The presence of forests can affect the water cycle through their high absorption of solar radiation due to low albedo, resulting in energy available for evapotranspiration of water, cloud formation and possible local showers (Scheffer et al., 2005).

In Eastern Puerto Rico, the decrease in rainfall in the recent decade may be influenced by the Saharan Air Layer (SAL) intrusion in the island. In 2015, for example, the Caribbean registered the highest dust concentration from 1980 to 2016, while an increasing trend in dust mass concentration has been reported since 1991 (Hosannah et al., 2019). It is known that SAL peaks from late June to mid-August and can propagate westward across the Atlantic Ocean, bringing anomalously hot, dry air in the low to the middle troposphere (around 700 hPa), producing thermodynamically stable conditions and limiting rainfall in the insular Caribbean, in general, and in Puerto Rico, in particular (Kuciauskas et al., 2018; Mote et al., 2017). Therefore, with the increase in dust concentration in the recent decade, the orographic effect that plays an important role in keeping eastern Puerto Rico wetter than most of the island may have been suppressed.

However, local factors may have played an additional role in precipitation variability, with the observed rainfall increase in central-west Puerto Rico during the recent decade being related to local island processes such as surface heating, orographic uplift, and sea-breeze trade-wind convergence that can overcome drought and SAL episodes (Hosannah et al., 2019). These local variations in precipitation over Puerto Rico were well represented during the 2015 drought event, when the east was severely affected by drought (Miller and Ramseyer, 2020; Mote et al., 2017), while the western side had sites registering positive precipitation anomalies (Hosannah et al., 2019).

4.2. Drought years versus baseline climatology

Overall, the island had much less net infiltration during drought years, with areas in the south close to 0 mm yr^{-1}. When analyzing the relationship between rainfall, runoff, and AET (Fig. 10) over the island during the drought years, it is also possible to see that at least two-thirds of the rainfall was lost as AET, and the remaining third was divided between runoff and net infiltration. Past studies suggested that high AET is one of the primary reasons for the lack of surface water availability, the vulnerability to drought, and changes in groundwater recharge on small tropical islands (Gamble, 2004; Holding et al., 2016).

A recent study analyzing historical meteorological drought in Puerto Rico from 1950 to 2019 indicated a high frequency of monthly extreme drought conditions in the northeast of the island (Sorí et al., 2021). This is the region where we found the decrease in net infiltration to be greater than 400 mm yr^{-1} below the baseline period during drought years. We know that for drought years, such as 1994 and 2015, one of the reasons for the greater reduction in rainfall in eastern Puerto Rico was the intrusion of the SAL, as previously

discussed. The inhibition of rainfall produced by SAL was likely more intense over the mountainous regions of Puerto Rico due to the stable thermodynamic conditions that suppressed the orographic uplift, resulting in less local rainfall (Miller and Ramseyer, 2020; Mote et al., 2017).

Additionally, the drought events of 1994 and 2015 were also related to the positive phase of the North Atlantic Oscillation (NAO) that occurred during the winter preceding the SAL intrusion and the drought event (Mote et al., 2017). This contributed to a stronger North Atlantic subtropical high (NAHP) and stronger trader winds over Tropical North Atlantic, which could have helped to bring more dust from SAL events toward Puerto Rico. The greater intensity of the 1994 and 2015 droughts in Puerto Rico was registered in other studies (Álvarez-Berríos et al., 2018; Mote et al., 2017), and the water budget presented here (Fig. 9) suggested they also share a water deficit occurring in the prior year. This indicates that an imbalance in water before a year with low rainfall are ingredients that may result in intense droughts.

Although recent work indicated that intense drought events are becoming more common on the east side of the island and its rainforest in the Luquillo Mountains (Álvarez-Berríos et al., 2018; Mote et al., 2017), a recent study suggested that forested areas are more resilient than deforested areas when drought events occur (Hall et al., 2022). The authors demonstrated that forest cover increases water storage and hillslope infiltration that may reduce drought impacts on streamflow in Puerto Rico, "highlighting maintenance of forest cover as an important water management strategy to increase infiltration" (Hall et al., 2022).

It is also important to highlight the potential effects of drought on aquifers. The area in northern Puerto Rico, where net infiltration reduction occurred, is situated above the North Coast Limestone Aquifer (Fig. 2**b**), which indicates a substantial reduction in groundwater recharge during drought events. The North Coast Limestone Aquifer is considered the most extensive and productive freshwater aquifer on the island, with its groundwater serving as an important source for local ecosystems and public water supply (Lugo et al., 2001; Maihemuti et al., 2015; Padilla et al., 2011). Therefore, the reduced rainfall in north and central Puerto Rico during drought years (Fig. 11 **b**) may directly affect the recharge of the North Coast Aquifer because parts of this aquifer are almost exclusively recharged by direct rainfall, while other areas are recharged both by direct rainfall and the streams from Cordillera Central (on the volcanic rocks) that infiltrate underground when they cross onto the karst areas (Mendez-Tejeda et al., 2016).

Differences in net infiltration in southern Puerto Rico, where the South Coast Aquifer is located, were smaller than on the rest of the island (≤ -100 mm yr^{-1}) during drought years when compared to the baseline climatology. This aquifer is also recharged by direct rainfall and streams flowing out of the Cordillera Central (Mendez-Tejeda et al., 2016). Therefore, the impacts of drought in the South Coast Aquifer recharge may come not only from the reduction in local rainfall and net infiltration but also from the decreased rainfall felt in central Puerto Rico, which affected the mountainous river's streamflow. Southeastern Puerto Rico was classified as the area of the island most exposed to any classification of drought from 2000 to 2016 (Álvarez-Berríos et al., 2018), while some studies indicated that the South Coast Aquifer has already been suffering from lower recharge and higher groundwater demand in the recent decade (Harmsen, 2019; Torres-Gonzalez and Rodriguez, 2016).

Moreover, the South Coast Aquifer's groundwater was the principal source of potable water for cities along the southern coast of Puerto Rico and the primary source of water for agricultural irrigation (Torres-Gonzalez and Rodriguez, 2016). Therefore, the lack of net infiltration and groundwater recharge during drought events (when surface water is limited) creates severe water stress. While one solution would be to develop energy-intensive desalination plants as an alternative water supply, this creates additional problems as desalinization is based on the use of fossil fuels; increased use of desalinization would increase air pollution and emissions of greenhouse gasses in the island (Mendez-Tejeda et al., 2016).

5. Conclusions

This study analyzed how the physical geography of Puerto Rico affects the island's water budget during a baseline climatology (1981–2010), a recent decade (2010–2019), and drought years (1991, 1994, 1997, and 2015). Results indicated that central-west, north, and eastern Puerto Rico had greater net infiltration than the south during baseline climatology and the recent decade. The greatest net infiltration occurred in mountainous and highly vegetated areas of the island, such as the Cordillera Central and the Luquillo Mountains, highlighting the important role of topography in creating orographic rainfall and vegetation as a source of moisture. The presence of group B and C soils, with higher infiltration rates, may have also contributed to the greater amount of net infiltration in those areas.

However, rainfall variability in the recent decade has affected the net infiltration, with the central-west and northern Puerto Rico receiving more rainfall, followed by greater net infiltration, and the east registering a decrease in both variables, which could be a consequence of large-scale atmospheric circulation mechanisms. Meanwhile, Southern Puerto Rico experienced lower net infiltration during both analysis periods. The location of the south, on the leeward side of the Cordillera Central, together with the presence of more group D soils (with lower infiltration rates), and greater areas of cultivated crops than natural vegetation, may have all combined to cause lower net infiltration there.

During drought years, the entire island reduced its net infiltration as a consequence of reduced rainfall, with the worst scenarios occurring in the central-west and eastern Puerto Rico (potentially affecting tropical forests and their soil moisture) as well as in parts of the north (where the productive North Coast Aquifer is located). While reductions in net infiltration during drought events were less dramatic in southern Puerto Rico than in other areas of the island, these reductions aggravated the persistent water stress by reducing recharge in the South Coast Aquifer, which already suffers from low recharge and high groundwater demand.

These findings are the first that we know of to highlight the role of physical geography on Puerto Rico's water budget and net infiltration while comparing the baseline climatology, the recent decade, and drought years. Thus, we expect they will be useful to help the local government in planning for water management and drought events. Moreover, we showed that SWB2, a newly released, open-

source water budget model, provides a useful platform for incorporating the physical geography of a tropical oceanic island in water planning and management. Even without calibration, the model performed satisfactorily, and very well in some cases, in matching observed streamflow from watersheds across Puerto Rico. This suggests that the model is suitable for use on other oceanic islands in tropical settings where data suitable for model calibration are lacking.

Finally, the authors note the limitations of the SWB2 model, mainly in reproducing low flows. Therefore, we suggest that future work should test the SWB2 model performance in Puerto Rico using different model parameters we have used here and even testing different datasets, as well as adding input data we did not find by the time of this research, such as fog interception or irrigation. The application of the SWB2 model in other Caribbean islands would also be interesting and allow for the comparison of SWB2 performance in different areas of the Caribbean.

Funding

This work was supported by the NSF Luquillo Long-Term Ecological Research Program (DEB1239764) and NOAA Modeling, Analysis, Predictions, and Projections (MAPP) grant (NA20OAR4310415).

CRediT authorship contribution statement

Flavia D.S. Moraes: Conceptualization; Data curation; Formal analysis; Investigation; Methodology; Software; Validation; Visualization; Writing – original draft; Writing – review & editing. **Thomas L. Mote:** Conceptualization; Funding acquisition; Project administration; Resources; Supervision; Validation; Writing – review & editing. **Todd C. Rasmussen:** Methodology; Supervision; Validation; Writing – review & editing.

Declaration of Competing Interest

The authors declare that they have no known competing financial interests or personal relationships that could have appeared to influence the work reported in this paper.

Data availability

All links to my data are available in the manuscript.

Acknowledgments

The authors thank Lucas Favero for supporting watershed evaluation and SWB2 analyses, as well as with valuable suggestions that helped improve this manuscript; Stephen Westenbroek from the U.S. Geological Survey for creating the SWB2 (https://pubs.er.usgs.gov/publication/tm6A59) and providing technical support for model execution; and Ayan Fleischmann for helping with MatLab coding. The authors also thank the NSF Luquillo Long-Term Ecological Research Program (DEB1239764) and NOAA Modeling, Analysis, Predictions and Projections (MAPP) grant (NA20OAR4310415) for funding this research. Finally, we thank Eric Harmsen for the GOES-PRWEB model data and thoughtful discussion about model outputs, as well as the National Aeronautics and Space Administration (NASA) for Daymet (version 3) daily precipitation data, the U.S. Geological Survey (USGS) for Puerto Rico streamflow data and SWB2.0 model, the Gridded Soil Survey Geographic (gSSURGO) Database for available water capacity and soil type data, the National Land Cover Database for Puerto Rico 2001 land use and land cover data, and NOAA Office for Coastal Management (NOAA/OCM) for Puerto Rico 2010 land use and land cover data.

Author statement

This work has not been published previously, it is not under consideration for publication elsewhere, its publication is approved by all authors and tacitly or explicitly by the responsible authorities where the work was carried out, and that, if accepted, it will not be published elsewhere in the same form, in English or in any other language, including electronically without the written consent of the copyright-holder.

Appendix A. Supporting information

Supplementary data associated with this article can be found in the online version at doi:10.1016/j.ejrh.2023.101382.

References

Álvarez-Berríos, N.L., Soto-Bayó, S., Holupchinski, E., Fain, S.J., Gould, W.A., 2018. Correlating drought conservation practices and drought vulnerability in a tropical agricultural system. Renew. Agric. Food Syst. 33 (3), 279–291. https://doi.org/10.1017/s174217051800011x.

Ang, R., Oeurng, C., 2018. Simulating streamflow in an ungauged catchment of Tonlesap Lake Basin in Cambodia using soil and water assessment tool (SWAT) model. Water Sci. 32 (1), 89–101. https://doi.org/10.1016/j.wsj.2017.12.002.
Ault, T., 2016. Island water stress. Nat. Clim. Change 6 (12), 1062–1063. https://doi.org/10.1038/nclimate3171.
Brewington, L., Keener, V., Mair, A., 2019. Simulating land cover change impacts on groundwater recharge under selected climate projections, Maui, Hawai'i. Remote Sens. 11 (24), 3048. https://doi.org/10.3390/rs11243048.
Cashman, A., Nurse, L., John, C., 2010. Climate change in the Caribbean: the water management implications. J. Environ. Dev. 19 (1), 42–67. https://doi.org/10.1177/1070496509347088.
Day, E.S., 2019. Application of the USGS soil-water-balance (SWB) model to estimate spatial and temporal aspects of groundwater recharge in north-central Iowa (Unpublished MS Thesis). Iowa State University,, Ames, IA (Unpublished MS Thesis). ⟨https://dr.lib.iastate.edu/handle/20.500.12876/31847⟩.
Dieter, C.A., Maupin, M.A., Caldwell, R.R., Harris, M.A., Ivahnenko, T.I., Lovelace, J.K., Barber, N.L., Linsey, K.S., 2018. Estimated use of water in the United States in 2015: U.S. Geol. Surv. Circ. 1441, 65. https://doi.org/10.3133/cir1441.
Farrell, D., Trotman, A., & Cox, C. (2010). Drought early warning and risk reduction. Global Assessment Report on Disaster Risk Reduction. ⟨https://www.preventionweb.net/english/hyogo/gar/2011/en/bgdocs/Farrell_et_al_2010.pdf⟩.
Gamble, D.W., 2004. Water Resource Development on Small Carbonate Islands: Solutions Offered by the Hydrologic Landscape Concept. In: Janelle, D.G., Warf, B., Hansen, K. (Eds.), WorldMinds: Geographical Perspectives on 100 Problems: Commemorating the 100th Anniversary of the Association of American Geographers 1904–2004. Springer, Netherlands, pp. 503–507. https://doi.org/10.1007/978-1-4020-2352-1_82.
Garcia-Martino, A.R., Warner, G.S., Scatena, F.N., Civco, D.L., 1996. Rainfall, runoff and elevation relationships in the Luquillo Mountains of Puerto Rico. Caribb. J. Sci. 32, 413–424. ⟨https://www.recursosaguapuertorico.com/Andres_Garcia_LEF_climate_paper_1996_CJS.pdf⟩.
Gassman, P.W., Reyes, M.R., Green, C.H., Arnold, J.G., 2007. The soil and water assessment tool: historical development, applications, and future research directions. Trans. ASABE 50 (4), 1211–1250. https://doi.org/10.13031/2013.23637.
Geoghegan, T., Renard, Y., 2002. Beyond community involvement: lessons from the insular Caribbean. Parks 12 (2), 16–27.
Hall, J., Scholl, M., Gorokhovich, Y., Uriarte, M., 2022. Forest cover lessens the impact of drought on streamflow in Puerto Rico. Hydrol. Process. 36 (5), e14551.
Hargreaves, G.H., Samani, Z.A., 1985. Reference crop evapotranspiration from temperature. Appl. Eng. Agric. 1 (2), 96–99. https://doi.org/10.13031/2013.26773.
Harlow, J., Hagedorn, B., 2018. SWB modeling of groundwater recharge on Catalina island, California, during a period of severe drought. Water 11 (1), 58. https://doi.org/10.3390/w11010058.
Harmsen, E.W. (2019, July 12, 2019). Puerto Rico South Coast Aquifer Recharge Analysis Press conference presentation, Central Office of the Autoridad de Acueductos y Alcantarillados, San Juan, PR. ⟨https://academic.uprm.edu/hdc/HarmsenPapers/Aquifer%20Recharge%20Analysis%20of%20Puerto%20Rico%20South%20Coast-Harmsen.pdf⟩.
Harmsen, E.W., Mecikalski, J.R., Reventos, V.J., Álvarez Pérez, E., Uwakweh, S.S., Adorno García, C., 2021. Water and energy balance model GOES-PRWEB: development and validation. Hydrology 8 (3), 113. https://doi.org/10.3390/hydrology8030113.
Healy, R.W., 2010. Estimating groundwater recharge. Cambridge University Press, p. 256. ISBN 978-0521863964.
Hendry, M.D., 1996. The geological legacy of small islands at the caribbean-atlantic boundary. Coast. Estuar. Stud. 205–224. https://doi.org/10.1029/CE051p0205.
Herrera, D., Ault, T., 2017. Insights from a new high-resolution drought atlas for the Caribbean spanning 1950–2016. J. Clim. 30 (19), 7801–7825. https://doi.org/10.1175/JCLI-D-16-0838.1.
Herrera, D.A., Ault, T.R., Fasullo, J.T., Coats, S.J., Carrillo, C.M., Cook, B.I., Williams, A.P., 2018. Exacerbation of the 2013–2016 Pan-Caribbean Drought by Anthropogenic Warming, 619-610,626 Geophys. Res. Lett. 45 (19), 10. https://doi.org/10.1029/2018gl079408.
Holding, S., Allen, D.M., Foster, S., Hsieh, A., Larocque, I., Klassen, J., Van Pelt, S.C., 2016. Groundwater vulnerability on small islands. Nat. Clim. Change 6 (12), 1100–1103. https://doi.org/10.1038/nclimate3128.
Holdridge, L.R. (1967). Life zone ecology. Tropical Science Center, San Jose, Costa Rica, 206 pp.
Hosannah, N., González, J.E., Lunger, C., Niyogi, D., 2019. Impacts of local convective processes on rain on the Caribbean island of puerto rico. J. Geophys. Res.: Atmospheres 124 (12), 6009–6026. https://doi.org/10.1029/2018jd029825.
Huffman, R.L., Fangmeier, D.D., Elliot, W.J., Workman, S.R., Schwab, G., 2011. Soil and water conservation engineering. Am. Soc. Agric. Biol. Eng. St. Joseph. 523.
Jury, M.R., 2020. Resolution-dependent perspectives on caribbean hydro-climate change. Hydrology 7 (4), 93. https://doi.org/10.3390/hydrology7040093.
Jury, M.R., 2022. Inter-comparison of past and projected climatic trends in Puerto Rico: 1950–2100. J. Water Clim. Change 13 (7), 2713–2724. https://doi.org/10.2166/wcc.2022.071.
Karnauskas, K.B., Schleussner, C.-F., Donnelly, J.P., Anchukaitis, K.J., 2018. Freshwater stress on small island developing states: population projections and aridity changes at 1.5 and 2 °C. Reg. Environ. Change 18 (8), 2273–2282. https://doi.org/10.1007/s10113-018-1331-9.
Keellings, D., Hernández Ayala, J.J., 2019. Extreme rainfall associated with hurricane maria over puerto rico and its connections to climate variability and change. Geophys. Res. Lett. 46 (5), 2964–2973. https://doi.org/10.1029/2019GL082077.
Kent, K., 1973. *A method for estimating volume and rate of runoff in small watersheds*.USDA Soil Conservation Service. SCS-TP-149 83.
Kuciauskas, A.P., Xian, P., Hyer, E.J., Oyola, M.I., Campbell, J.R., 2018. Supporting Weather Forecasters in Predicting and Monitoring Saharan Air Layer Dust Events as They Impact the Greater Caribbean. Bull. Am. Meteorol. Soc. 99 (2), 259–268. https://doi.org/10.1175/bams-d-16-0212.1.
Kumar, N., Singh, S.K., Srivastava, P.K., Narsimlu, B., 2017. SWAT Model calibration and uncertainty analysis for streamflow prediction of the Tons River Basin, India, using Sequential Uncertainty Fitting (SUFI-2) algorithm. Model. Earth Syst. Environ. 3 (1), 30. https://doi.org/10.1007/s40808-017-0306-z.
Lim, K.J., Engel, B.A., Tang, Z., Choi, J., Kim, K.S., Muthukrishnan, S., Tripathy, D., 2005. Automated web GIS based hydrograph analysis tool, WHAT 1. J. Am. Water Resour. Assoc. 41 (6), 1407–1416. https://doi.org/10.1111/j.1752-1688.2005.tb03808.x.
Lugo, Ariel E., Leopoldo Miranda Castro, Abel Vale, Tania del Mar López, Enrique Hernández Prieto, Andrés García Martinó, Alberto R. Puente Rolón, Adrianne G. Tossas, Donald A. McFarlane, Tom Miller, Armando Rodríguez, Joyce Lundberg, John Thomlinson, José Colón, Johannes H. Schellekens, Olga Ramos, Eileen Helmer (2001) Puerto Rican Karst-A Vital Resource. USDA Forest Service, General Technical Report WO-65. ⟨https://scholarship.claremont.edu/cgi/viewcontent.cgi?article=1020&context=wmkeckscience⟩.
Maihemuti, B., Ghasemizadeh, R., Yu, X., Padilla, I., Alshawabkeh, A.N., 2015. Simulation of Regional Karst Aquifer System and Assessment of Groundwater Resources in Manatí-Vega Baja, Puerto Rico. J. Water Resour. Prot. 07 (12), 909–922. https://doi.org/10.4236/jwarp.2015.712075.
Martinez, C., Goddard, L., Kushnir, Y., Ting, M., 2019. Seasonal climatology and dynamical mechanisms of rainfall in the Caribbean [journal article]. Clim. Dyn. https://doi.org/10.1007/s00382-019-04616-4.
Mecikalski, J.R., & Harmsen, E.W. (2019). The Use of Visible Geostationary Operational Meteorological Satellite Imagery in Mapping the Water Balance over Puerto Rico for Water Resource Management. In. IntechOpen. https://doi.org/10.5772/intechopen.82460.
Mendez-Tejeda, R., Richards, R., Emiliano, A., 2016. Anal. Groundw. Puerto Rico 4, 68–76. https://doi.org/10.12691/ajwr-4-3-3.
Miller, J.A., Whitehead, R., Oki, D.S., Gingerich, S.B., Olcott, P.G., 1997. Ground Water Atlas of the United States: Segment 13, Alaska, Hawaii, Puerto Rico, and the US Virgin Islands. US Geol. Surv. Hydrol. Atlas 730-N. https://doi.org/10.3133/ha730N.
Miller, P.W., Ramseyer, C.A., 2020. Did the climate forecast system anticipate the 2015 Caribbean Drought? J. Hydrometeorol. 21 (6), 1245–1258. https://doi.org/10.1175/jhm-d-19-0284.1.
Miller, P.W., Kumar, A., Mote, T.L., Moraes, F.D.S., Mishra, D.R., 2019. Persistent Hydrological Consequences of Hurricane Maria in Puerto Rico. Geophys. Res. Lett. 46 (3), 1413–1422. https://doi.org/10.1029/2018GL081591.
Miller, P.W., Williams, M., Mote, T., 2021. Modeled atmospheric optical and thermodynamic responses to an exceptional trans-atlantic dust outbreak. e2020JD032909 J. Geophys. Res.: Atmospheres 126 (5). https://doi.org/10.1029/2020JD032909.
Moraes, F.D.S., Mote, T.L., Seymour, L., 2022. Ocean–atmosphere variability and drought in the insular Caribbean. Int. J. Climatol. 42 (10), 5016–5037. https://doi.org/10.1002/joc.7517.
Moriasi, D.N., Arnold, J.G., Van Liew, M.W., Bingner, R.L., Harmel, R.D., Veith, T.L., 2007. Model evaluation guidelines for systematic quantification of accuracy in watershed simulations. Trans. ASABE 50 (3), 885–900. https://doi.org/10.13031/2013.23153.

Mote, T.L., Ramseyer, C.A., Miller, P.W., 2017. The Saharan air layer as an early rainfall season suppressant in the Eastern Caribbean: The 2015 Puerto Rico drought. J. Geophys. Res.: Atmospheres 122 (20). https://doi.org/10.1002/2017JD026911.

Padilla, I., Irizarry, C., Steele, K., 2011. Historical contamination of groundwater resources in the North Coast Karst Aquifers of Puerto Rico. Dimens. Ing. Y. Agrimens. CIAPR 3, 7–12. ⟨https://www.ncbi.nlm.nih.gov/pmc/articles/PMC3999440/⟩.

Ramseyer, C.A., Mote, T.L., 2018. Analysing regional climate forcing on historical precipitation variability in Northeast Puerto Rico. Int. J. Climatol. 38 (S1), e224–e236. https://doi.org/10.1002/joc.5364.

Scheffer, M., Holmgren, M., Brovkin, V., Claussen, M., 2005. Synergy between small- and large-scale feedbacks of vegetation on the water cycle. Glob. Change Biol. 11 (7), 1003–1012. https://doi.org/10.1111/j.1365-2486.2005.00962.x.

Sobel, A.H., Burleyson, C.D., Yuter, S.E., 2011. Rain on small tropical islands. J. Geophys. Res. 116 (D8) https://doi.org/10.1029/2010jd014695.

Sorí, R., Méndez-Tejeda, R., Stojanovic, M., Fernández-Alvarez, J.C., Pérez-Alarcón, A., Nieto, R., Gimeno, L., 2021. Spatio-Temporal Assessment of Meteorological Drought in Puerto Rico between 1950 and 2019. Environ. Sci. Proc. 8 (1), 40. ⟨https://www.mdpi.com/2673-4931/8/1/40⟩.

Thornthwaite, C.W. & Mather, J.R. (1957). Instructions and tables for computing potential evapotranspiration and the water balance. Laboratory of Climatology, Centerton, New Jersey.

Thornton, P.E., Thornton, M.M., Mayer, B.W., Wei, Y., Devarakonda, R., Vose, R.S., & Cook, R.B. (2016). Daymet: Daily Surface Weather Data on a 1-km Grid for North America, Version 3. In: ORNL Distributed Active Archive Center. ⟨https://daac.ornl.gov/DAYMET/guides/Daymet_Daily_V4.html⟩.

Torres-Gonzalez, S., & Rodriguez, J.M. (2016). Hydrologic conditions in the South Coast aquifer, Puerto Rico, 2010–15 [Report](2015–1215). (Open-File Report, Issue. U. S. G. Survey. ⟨http://pubs.er.usgs.gov/publication/ofr20151215⟩.

Torres-Valcárcel, Á., Harbor, J., González-Avilés, C., Torres-Valcárcel, A., 2014. Impacts of urban development on precipitation in the tropical maritime climate of Puerto Rico. Climate 2 (2), 47–77. https://doi.org/10.3390/cli2020047.

USDA (2020). Gridded Soil Survey Geographic (gSSURGO) Database for the United States of America and the Territories, Commonwealths, and Island Nations served by the USDA-NRCS. ⟨https://data.nal.usda.gov/dataset/gridded-soil-survey-geographic-database-gssurgo⟩.

Westenbroek, S.M., Kelson, V.A., Dripps, W.R., Hunt, R.J., & Bradbury, K.R. (2010). SWB-A modified Thornthwaite-Mather Soil-Water-Balance code for estimating groundwater recharge [Report](6-A31). (Techniques and Methods, Issue. U. S. G. Survey. ⟨http://pubs.er.usgs.gov/publication/tm6A31⟩.

Westenbroek, S.M., Engott, J.A., Kelson, V.A., & Hunt, R.J. (2018). SWB Version 2.0—A soil-water-balance code for estimating net infiltration and other water-budget components. US Geological Survey Techniques and Methods 6A-59, ⟨http://pubs.er.usgs.gov/publication/tm6A59⟩.

Xu, Z. (2016). Data analysis and numerical modeling of seawater intrusion through conduit network in a coastal karst aquifer. Unpublished PhD dissertation, The Florida State University, Tallahassee, Florida, 112 pp. ⟨http://purl.flvc.org/fsu/fd/FSU_2016SP_Xu_fsu_0071E_13049⟩.

Zhang, L., Sun, G., Cohen, E., McNulty, S.G., Caldwell, P.V., Krieger, S., Christian, J., Zhou, D., Duan, K., Cepero-Pérez, K.J., 2018. An improved water budget for the El Yunque National Forest, Puerto Rico, as determined by the water supply stress index model. For. Sci. 64 (3), 268–279. https://doi.org/10.1093/forsci/fxx016.